TECHNISCHE UNIVERSITÄT DRESDEN

FACULTY OF COMPUTER SCIENCE
INSTITUTE OF SOFTWARE AND MULTIMEDIA TECHNOLOGY
CHAIR OF COMPUTER GRAPHICS AND VISUALIZATION
PROF. DR. STEFAN GUMHOLD

Bachelor's Thesis

for obtaining the academic degree
Bachelor of Science

Development of a Natural VR User Interface Using Haptic Gloves

Lucas Waclawczyk
(Born 26. April 1998 in Bad Langensalza, Mat.-No.: 4686687)

Tutor: Prof. Stefan Gumhold

Dresden, September 4, 2020

Task Description

Write down your task...

Declaration of authorship

I hereby declare that I wrote this thesis on the subject

Development of a Natural VR User Interface Using Haptic Gloves

independently. I did not use any other aids, sources, figures or resources than those stated in the references. I clearly marked all passages that were taken from other sources and cited them correctly.

Furthermore I declare that – to my best knowledge – this work or parts of it have never before been submitted by me or somebody else at this or any other university.

Dresden, September 4, 2020

Lucas Waclawczyk

Kurzfassung

abstract text german

Abstract

abstract text english

Contents

1 Introduction **4**

1.1 Principles of Data Gloves 4

1.2 Examples and Applications of Data Gloves 5

1.2.1 Sign Language Recognition 5

1.2.2 Daily Activity Recognition 7

1.2.3 Refined Myoelectric Control in Below-Elbow Amputees 8

1.2.4 A Lightweight Force-Feedback Glove 9

1.2.5 Commercial Products 11

2 Development **13**

2.1 Devices and Software 13

2.2 Skeletal Hand Model for the Avatar VR Haptic Glove 15

2.2.1 Abstraction of the Human Hand Skeleton 15

2.2.2 Technology and Function of the Avatar VR 15

2.2.3 Using Data From the Avatar VR to Visualize the User's Hand 17

2.3 Project Idea and Structure 18

2.3.1 Main class 20

2.3.2 Bridge 20

2.3.3 Space, Targets and Phasers 20

2.3.4 Control Panel 21

2.3.5 Hands 21

2.3.6 Headup Display 21

2.4 Calibration 22

2.5 Space, Targets and Phasers 24

3 Evaluation **28**

3.1 Participating Subjects and Preparation 28

3.2 Qualitative Evaluations and Suggestions 28

Bibliography **32**

1 Introduction

In their review *Haptic display for virtual reality: progress and challenges*[WGL+19], Wang et al. state that Virtual Reality (VR) was born in 1965 with Ivan Sutherlands proposal of a concept named "The Ultimate Display"[Sut65]. In that report of the IFIP Congress, Sutherland names immersion, interaction and imagination as three important features of VR.

There has been a multitude of approaches to making interaction with virtual environments possible[LHT+19]. Touch screens and stylus pens have become quite common in everyday life. Devices capable of capturing scene depth like Microsoft Kinect and Leap Motion make touchless interaction possible, e.g. during games. This thesis focuses especially on wearable devices called *data gloves*.

1.1 Principles of Data Gloves

The general principles of data gloves can be divided into two main parts: sensing and actuation. The first part deals with the issue of capturing a user's hand poses and motions and relaying that information to a computer for further processing. In most cases, a fabric glove is equipped with an intertial measurement unit (IMU) placed on each rigid hand part or flex sensors placed on joints. The latter have the advantage of measuring absolute values which, however, are only scalar and need further interpretation involving anatomical knowledge ("Something is happening: we have a .7."). An intertial measurement unit (IMU), on the other hand, usually accumulates an absolute measurement from instantaneous rates of change, but can be designed to return 3D rotations and positions ("The index is facing upwards.").

The matter of actuation belongs to the broader field of haptic feedback. According to Wang et al.[WGL+19], the visual and auditory feedback of VR systems has become fairly realistic over time. However, haptic feedback is still rather poor even though it is "... indespensable for enhancing immersion, interaction and imagination of VR systems. Interaction can be enhanced by haptic feedback as users can directly manipulate virtual objects, and obtain immediate haptic feedback. Immersion of the VR system can be enhanced in terms of providing more realistic sensation to mimic the physical interaction process. Imagination of users can be inspired when haptics can provide more cues for user[s] to mentally construct an imagined virtual world beyond spatial and or temporal limitations."

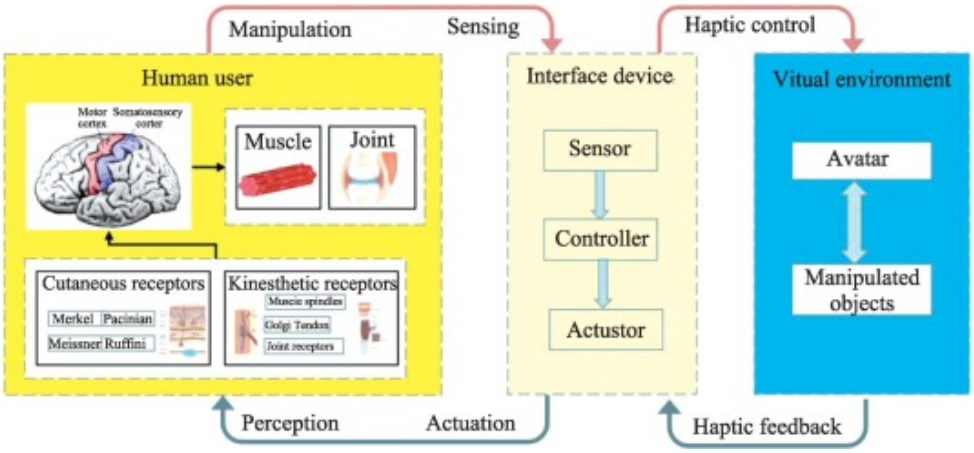

Figure 1.1: Schematic paradigm of haptic human computer interfaces consisting of three components, i. e. human user, interface device, and virtual environment; from [WGL+19]

A schematic of the general paradigm of haptic human computer interfaces is shown in figure 1.1. It consists of three main components:

- the user, who perceives virtual objects through biological receptors, processes them in the somatosensory and motor cortex, and requests manipulation by mechanical movement,
- the interface device which causes perception via actuation and collects information about requested manipulation with its sensors,
- the virtual environment which evaluates the interface device's data, realizes the manipulation of virtual objects with possible constraints, and motivates actuation in the interface device via haptic feedback.

As the following examples will demonstrate, not all data gloves are designed with the capability of both sensing and actuation. Some are only used to evaluate the user's hand pose, and it is conceivable to deal only with the issue of actuation and utilize an external device for sensing, such as Leap Motion. However, actuation on its own does not seem useful for VR applications, as it needs to be variable based on the current hand pose for which tracking of the user's hand pose is required.

1.2 Examples and Applications of Data Gloves

1.2.1 Sign Language Recognition

In 2018, Kakoty et al. developed a data glove and processing system for the recognition of sign language alphabets (Indian, American and numbers) and their translation into speech[KS18]. In their paper, several earlier projects with similar purposes are reviewed, most of which are vision based. The authors point out

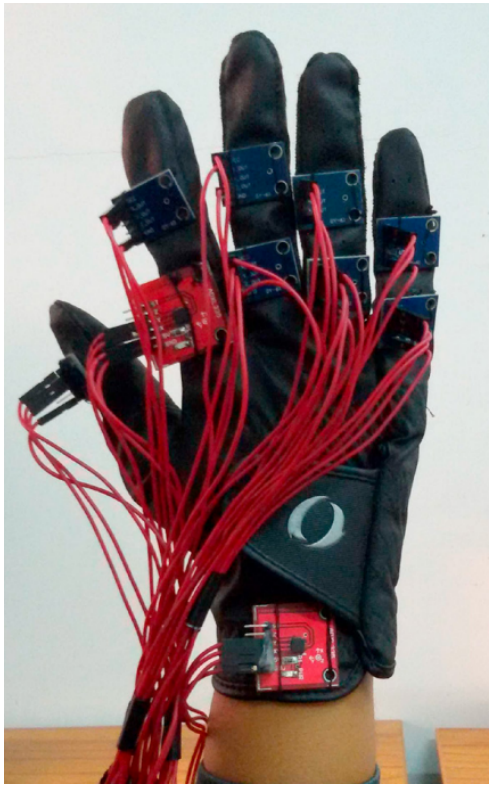

(a) Data glove developed by Kakoty et al.

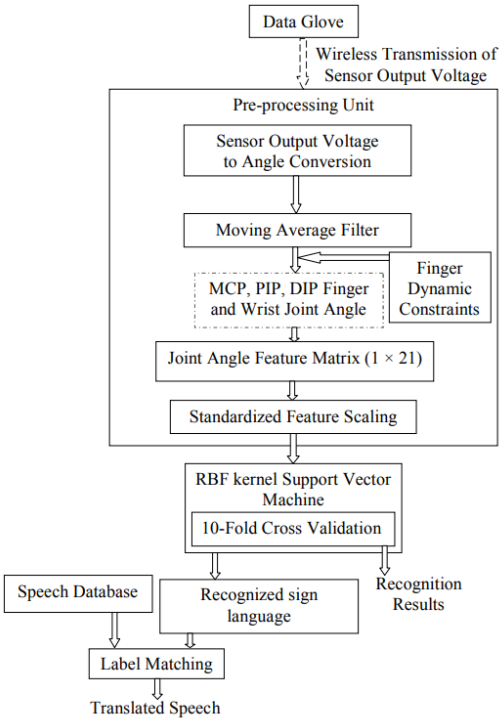

(b) Proposed methodology for sign language recognition

Figure 1.2: A system for sign language recognition; from [KS18]

that glove based systems are more useful because they "[. . .] allow one with the freedom for locomotion during the recognition process and [are] independent of the environmental lighting conditions."

The data glove used for this project is shown in figure 1.2a. It was constructed from a leather glove by equipping it with ten angle sensors, a microcontroller, and a transceiver module. The original paper describes this design in detail.

A preprocessing unit as in figure 1.2b handles the conversion from sensor output voltage to denoised, constrained standardized feature vectors. These are then processed by a radial base function kernel support vector machine and finally, the recognized sign language is translated into speech using label matching with a pre-recorded speech database. The whole process is implemented to run in real-time with the sensor data acquisition.

With an average recognition rate of 96.7%, this approach achieves similar results as previous projects while recognizing more alphabets. Kakoty et al. further conclude that their approach "[. . .] overcomes the limitations of vision based systems. [. . .] An extension of the presented work for sentence-based sign language recognition will lead to an enterprising device; which is part of on-going research."

(a) Arrangement of sensors on the hand

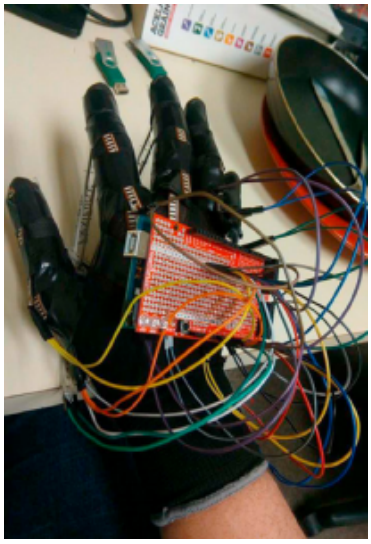

(b) Prototype device

Table 1. Object recognition with k-NN, 70-30.

k-NN, $k = 5$, Euclidean distance, 70-30				
Global Accuracy	0.94			
Global Cohen's Kappa	0.94			
	P	R	F	Support
Hold a plate	0.9960	0.9880	0.9920	251
Hold a cup	0.9246	0.9510	0.9376	245
Hold a spoon	0.9427	0.9030	0.9224	237
Hold a knife	0.9098	0.8657	0.8872	268
Hold a fork	0.8992	0.9612	0.9292	232
Hold a pot	0.9835	0.9715	0.9775	246
Hold a pall	0.9395	0.9902	0.9642	204
Empty hand	0.9600	0.9375	0.9486	256

Table 2. Object recognition with RF, 70-30.

RF, $T = 100$, $N = \sqrt{30}$, 70-30				
Global Accuracy	0.99			
Global Cohen's Kappa	0.99			
	P	R	F	Support
Hold a plate	1.0000	1.0000	1.0000	251
Hold a cup	0.9796	0.9796	0.9796	245
Hold a spoon	0.9957	0.9873	0.9915	237
Hold a knife	0.9703	0.9739	0.9721	268
Hold a fork	0.9744	0.9828	0.9785	232
Hold a pot	0.9959	0.9959	0.9959	246
Hold a pall	1.0000	1.0000	1.0000	204
Empty hand	1.0000	0.9961	0.9980	256

(c) Evaluation of the recognition results

Figure 1.3: A data glove for recognition of basic daily activities; from [MRB+19]

1.2.2 Daily Activity Recognition

Alzheimer's disease is a common cause for the loss of cognitive abilities amongst the elderly. Well known symptoms include language problems, loss of memory and degrading functioning of the hand. To better understand the latter, Maitre et al. investigated a method to recognize daily activities using a data glove developed over the course of the project[MRB+19].

Several reasons are named as motivation to develop the device from scratch:

- Prices for commercial data gloves are situated between ca. 600 USD and several thousand USD. The authors propose a design that can be recreated for only about 220 USD.
- Commercial gloves are generally only compatible with Windows, but the SDK is not suitable for many other sensors.

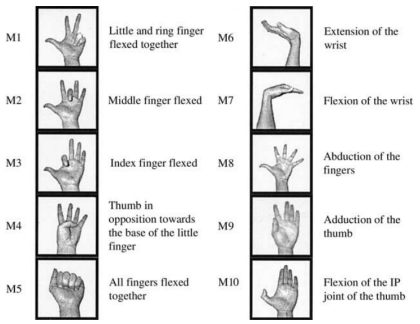

(a) Hand poses performed during training data acquisition

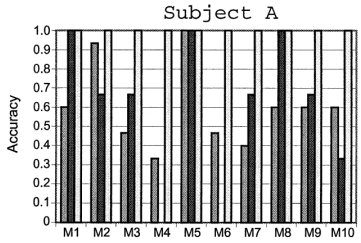

(b) Recognition results of phantom hand movements for a subject with traumatic amputation (Subject A)

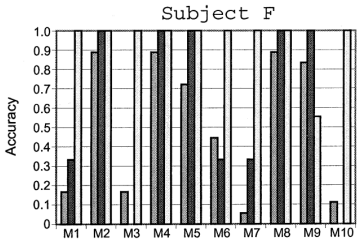

(c) Recognition results of phantom hand movements for a subject with congenital failure of formation (Subject F)

Figure 1.4: Hand poses used in [SRL05] and recognition results; in (b) and (c), grey bars depict average performance, black depicts best-session performance and white the reference glove performance

- The new design can be specialized for recognizing the required types of grasp.

Discerning a daily activity is based on recognizing the involved item, e.g. a plate for the task *Hold a plate*. For this, the presence of an object needs to be detected and information about its shape is required. Figure 1.3a shows the resulting sensor locations, where red and yellow mark flex sensors and blue marks force sensors. A prototype device can be seen in figure 1.3b.

A group of nine participants was asked to perform the daily activities listed in the evaluation tables in figure 1.3c. The acquired data sets were used to train (70%) and test (30%) a k Nearest Neighbours (k-NN) model whose precision (P), recall (R) and f-score (F) can be found in the left table, and a random forest (RF) to which the right table refers.

Maitre et al. conclude that the performance of their approach is "[. . .] almost perfect [. . .]. This result is surprising and encouraging [. . .]." Another experiment shows that both models perform significantly worse on data collected from a person that was not recorded during training. The authors therefore suggest to train the models with data from a patient that is supposed to use the system. The device can then even be worn in the comfort of the patient's home to monitor their hand activity.

1.2.3 Refined Myoelectric Control in Below-Elbow Amputees

A group of PhD students in Sweden trained an artificial neural network (ANN) to recognize myoelectric activity of below-elbow amputees as certain hand poses[SRL05]. To generate training data, a group of five subjects with a traumatic amputation and one subject with a congenital failure of formation was asked to perform the movements shown in figure 1.4a with their healthy hand and their phantom hand

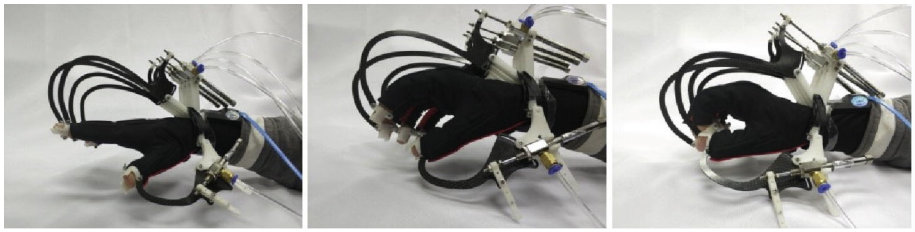

Figure 1.5: Physical prototype of a lightweight force-feedback glove with large workspace; from [ZWW+18]

simultaneously.

The healthy hand was therewhile tracked with a data glove to match the performed movement to one of M1 - M10. The arm stump on the side of the amputation was covered with considerably many electrodes to record detailed information about the remaining myoelectric activity. The (pre-processed) data was then used to train a tree-structured ANN.

As shown in figure 1.4 and more diagrams from the original paper, certain poses were recognized especially well or badly for certain subjects. An interesting process to see was how the performance of the subjects became more accurate over the course of the experiment. As this could be seen within minutes, the authors theorized, it might be due to unmasking of existing brain structures instead of the formation of new ones.

The subject with congenital failure was of special interest because it showed that some movements could be accurately induced in the phantom hand even though they had never been executed before, possibly indicating the awakening of sleeping motor cortical areas in the brain that had been present since birth. Among the subjects with traumatic amputations, the accuracy and training effect did not seem related to the time since the amputation.

An important aspect for the training effect might be the simultaneous execution of movements with the healthy hand, as suggested in the original paper. The authors moreover suppose that a subject's performance might increase with visual feedback of a virtual phantom hand that was not present during these experiments. This thesis might be useful for this purpose, as it describes the use of a well established hand model in section 2.2. Work in this direction was continued by the authors of the original paper[SEBL06].

1.2.4 A Lightweight Force-Feedback Glove

In terms of haptic feedback, a recent project is the *Design of a Lightweight Force-Feedback Glove with a Large Workspace*[ZWW+18]. From their review of existing technology, the authors of the respective paper

conclude the following "[. . .] requirements of ideal force feedback for VR interaction":

- The device weight should not exceed $100g$. This value is based on the success of desktop force-feedback devices, e.g. the PHANTOM Desktop. The prototype shown in figure 1.5 has a final mass of $245g$ which was achieved by a pneumatically actuated design with an outsourced construction for air compression and regulation. Force can be excerted onto the fingers by releasing compressed air into the pneumatic pistons (silver) which then pull back the links (black). Special materials were chosen for weight reduction: the links are made from $2mm$ thick carbon. Lightweight plastic was used for the base parts and finger caps (white).
- Typical grasping motions should be possible to simulate realistically. The device should therefor have a large motion and force range. The form of the links is specifically designed to ensure the necessary freedom of motion and makes it possible to mount the construction on the dorsal side of the hand. The authors emphasize that the key to obtaining optimal normal force at the finger cap while ensuring free movement of the finger joints is the curved profile of the sliding slot connecting the base components to the links. Its design and the respective calculations are described in detail in the original paper.
- "[. . .] the gloves should be easy to put on and remove, and should be adaptable for users with different hand sizes." This could, however, not be achieved and is suggested for future work.

A commercial data glove was used to track the user's hand. The pose was then evaluated by a PC that coordinated the release of air from the compression system into the pistons via a microcontroller.

Experiments showed that the prototype developed by the Zheng et al. can excert forces between $0.1N$ during free motion of the finger joints and $4N$ for constrained space simulation. It does indeed have a large working space in which a minimal virtual sphere with a diameter of $30mm$ can be simulated.

However, the normal force at the finger cap could not be controlled accurately. According to the authors, a possible solution might be the use of a force sensor at the finger tip to design a closed-loop control system. Moreover, the force-feedback showed significant delay due to the time of airflow between compression system and pistons.

For future work, the original paper suggests the development of new control hardware and software. They see the possibility of integrating the glove with a head mounted device (HMD) for novel applications such as e-shopping and plan to add components for haptic feedback on the hand palm as well.

Figure 1.6: Examples of commercial data gloves as named in table 1.1 (fltr, top-row first); from [WGL+19]

1.2.5 Commercial Products

Numerous types of data gloves have been available on the market over the past years. Some examples capable of haptic feedback are shown in figure 1.6 and a summary of their technological properties is compiled in table 1.1. Another example is the Avatar VR glove which will be used for the purposes of this thesis and explained in more detail in chapter 2.

Device name	Company	Motion tracking DoF	Force feedback	Tactile feedback	Actuation principle	Sensing principle	Typical features
CyberGrasp	Immersion	—	One actuator per finger	—	Electric motor	22-sensor CyberGlove device	Feel the size and shape
H-glove	Haption	Each finger posesses 3 DoF	Force feedback on 3 fingers	—	Electric motor	—	Can be attached to a Virtuose 6D
Dexmo	DextaRobotics	Tracking 11 DoF for hand	Force feedback on 5 fingers	Three linear resonant actuators	Electric motor	Rotary sensors	Feel the shape, size and stiffness
Haptx glove	Haptx	Tracking 6 DoF per digit	Lightweight exoskeleton applies up to $4lbs$ per finger	130 stimuli points	Microfluidic array	Magnetic tracking	Feel shape, texture, motion in sub-mm precision
Plexus	Plexus	21 DoF per hand	—	One tactile actuator per finger	—	Using tracing adapters for other technology	Track with .01 deg precision
VRgluv	VRgluv	12 DoF for the fingers on each hand	Apply up to $5lbs$ of varying force per finger	—	DC motors	5 sensors per finger	Simulate stiffness, shape, and mechanical features

Table 1.1: Existing commercial haptic feedback gloves; adapted, from [WGL+19]

2 Development

This chapter names the technology used for this project, defines a skeletal hand model for the Avatar VR haptic glove, and describes the development of a natural VR user interface based on these concepts.

2.1 Devices and Software

For the purpose of thesis, I used a pair of haptic gloves called Avatar VR which is a registered trademark of NeuroDigital Technologies, S. L.[nd], referred to as ND hereafter..

To use the Avatar VR on a computer, one needs to download, install and run the ND Suite. This program provides a background service and GUI for managing and accessing the devices. A connection can be established via Bluetooth after which all sensor data is graphically displayed in the GUI.

ND also supplies a developer's API in the form of three files (`NDAPI.h`, `NDAPI_x64.lib` and `NDAPI_x64.dll` or `x86` respectively) which need to be included in the project in a suitable manner. An instance of the `NDAPI.h` can be used to access the data of devices connected to ND Suite.

Additionally, a Vive tracker was used to determine the user's hand position and orientation. The Avatar VR can be mechanically connected to the tracker using a coupling that needs to be acquired separately. The devices named so far and the way of coupling them can be seen in figure 2.1.

The foundation for the graphics software I developed is implemented in the `cgv` framework provided by the chair of computer graphics and visualization at TU Dresden.

A user can view the plugin on a computer screen with the `cgv_viewer` or on a Vive head mounted device (HMD) simply by connecting one to the computer.

(a) Uncoupled devices, colors mark coupling points

(b) Coupled devices on user hand

Figure 2.1: Devices used to track the user's hand: Vive tracker, coupling, Avatar VR

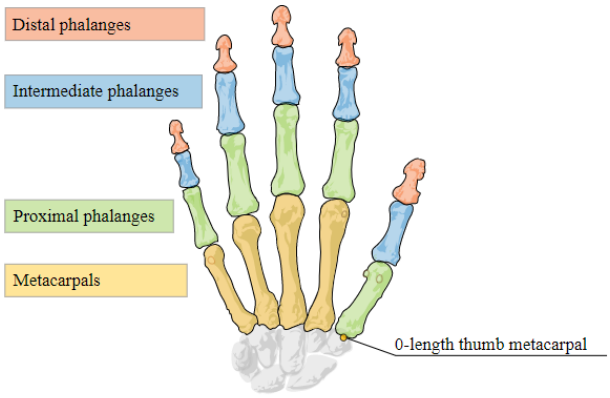

(a) General bone structure of the human hand

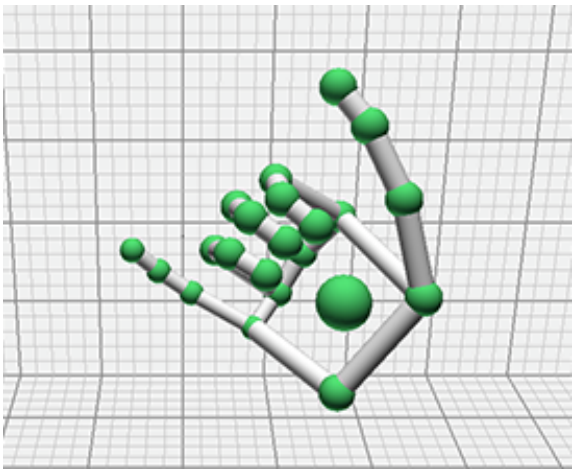

(b) Screenshot of an example hand representation in the Leap Motion API version 2.0, cropped

Figure 2.2: A model of the human hand; from [lea]

2.2 Skeletal Hand Model for the Avatar VR Haptic Glove

2.2.1 Abstraction of the Human Hand Skeleton

The human hand can be roughly divided into the parts shown in figure 2.2a, i.e. the *metacarpals*, *proximal phalanges*, *intermedial phalanges*, and *distal phalanges*. A joint connecting a metacarpal to a proximal phalanx is called *metacarpophalangeal joint*, and followed by a *proximal interphalangeal joint* and a *distal interphalangeal joint*.

Even though the carpals (grey in figure 2.2a) are physiologically quite relevant for hand movement, they stay relatively fixed compared to the other bone sets, and can thus be omitted in our simplified model. In anataomical nomenclature, the thumb is composed of proximal phalanx and distal phalanx only and follows a metacarpal. However, this model assumes a missing metacarpal and existing intermedial phalanx instead which will be modelled by a 0-length metacarpal for uniformity reasons.

The Leap Motion API version 2.0[lea] uses the abstraction described above and adds

- an "end" joint per finger (at the end of the distal phalanx)
- a joint diagonally across the palm from the metacarpophalangeal joint of the index
- a joint in the middle of the palm

The most common representation includes cylinders for the bones and spheres for the joints. It is shown in figure 2.2b.

2.2.2 Technology and Function of the Avatar VR

The Avatar VR is equipped with three kinds of sensors:

- An *intertial measurement unit (IMU)* is located on the intermedial phalanx of each finger to measure its 3D rotation. The thumb is even equipped with two IMUs (one per phalanx) and the palm with an IMU that can measure both 3D acceleration and 3D rotation. The "Motion" tab of ND Suite shown in figure 2.3a depicts the resulting orientations as orthonormal bases.
- At the locations marked in blue in figure 2.3b, the fabric is made of an electrically conductive material. These parts are used as contact sensors (short: contacts) to determine which of the marked locations are joined.
- The thumb has a flex sensor, that will not be relevant for this thesis.

Furthermore, there are actuators at the locations marked in blue in figure 2.3c. These can be used to generate vibrations of variable intensity as haptic feedback in a way that "[. . .] the brain perceives it as

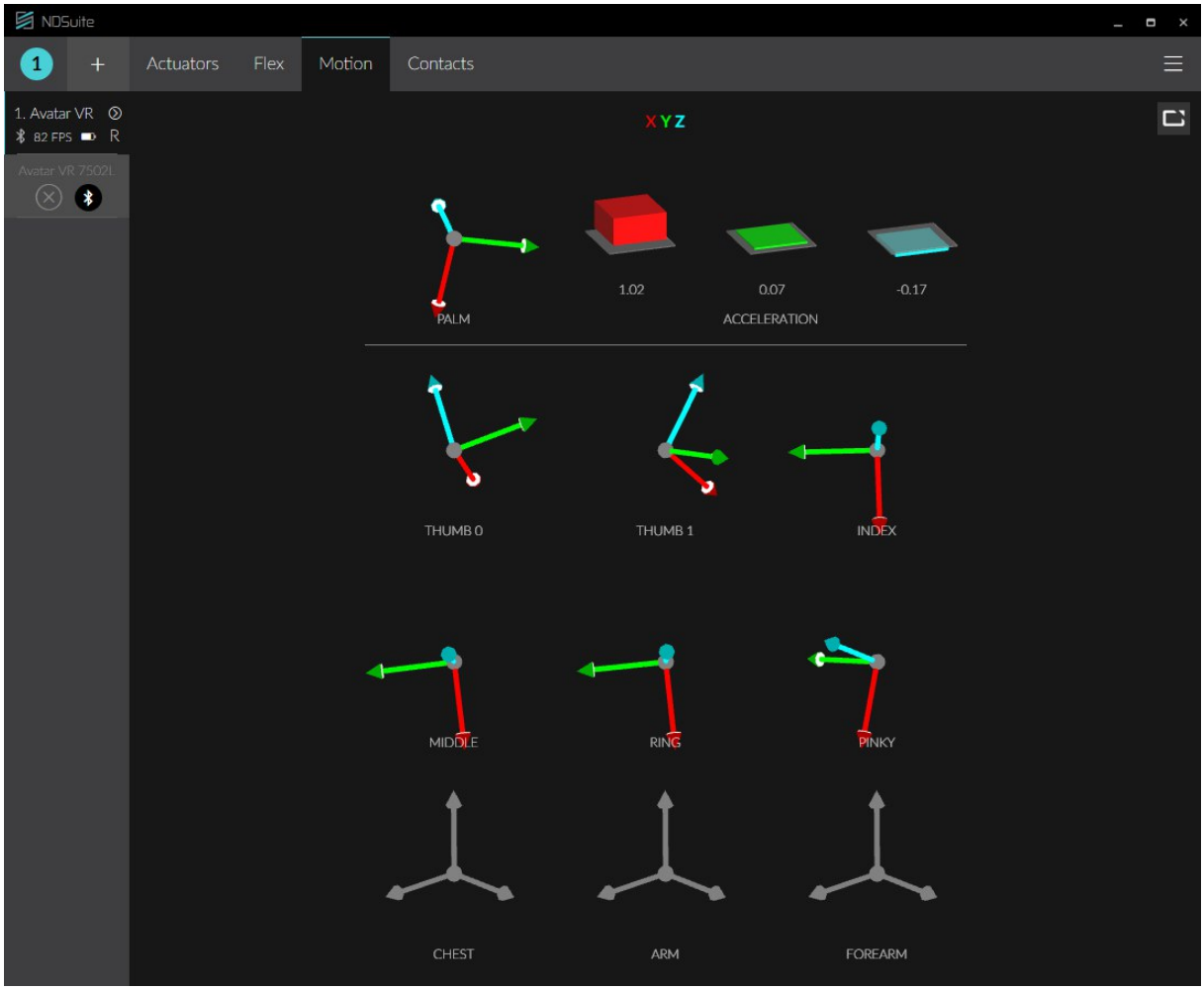

(a) "Motion" tab of ND Suite with orientations in an (optimistic) example hand pose

(b) Positions of contact sensors

(c) Positions of actuators

Figure 2.3: Sensors and actuators of the Avatar VR;
screenshots of ND Suite (b and c cropped)

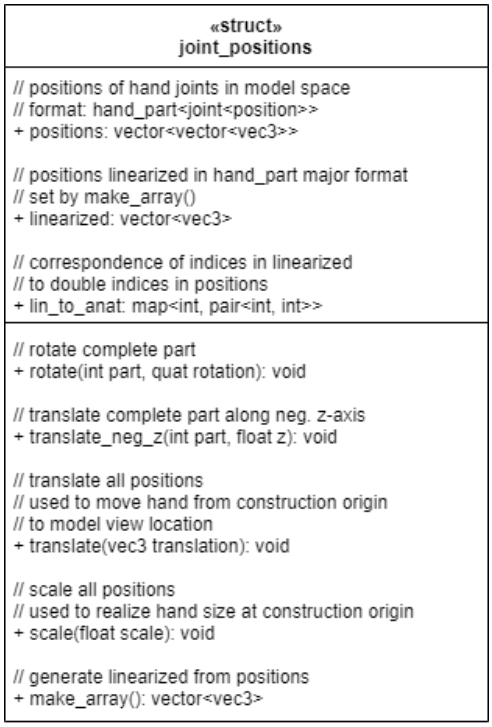

Figure 2.4: Struct for managing positions of hand joints, only most important parts included

'Real Touch' input", according to the producer.

2.2.3 Using Data From the Avatar VR to Visualize the User's Hand

The same model used by the Leap Motion API version 2.0 will also be used here. Leap captures absolute joint positions and optimizes them for visualization. In contrast, my approach for the Avatar VR is to use a fixed resting state geometry of the user's hand (bone lengths and resting state joint positions). At the time of a `draw()` command, the geometry is adjusted according to the data given by the glove and the Vive tracker. This is done with the help of the struct shown in figure 2.4 (only most important parts included).

First, the palm joints' positions are rotated according to the orientation given by the Vive tracker and saved in `positions`. The construction of each finger begins at the end joint of the distal phalanx which is initialized in `positions` as $(0, 0, 0)$, translated along the negative z-axis by the hard-coded length of the distal phalanx and rotated by the respective quaternion (see below). The other phalanges are constructed in the same manner, before the whole finger is translated to its metacarpophalangeal joint. Finally, the whole hand is scaled to model view space and translated to the model view position of the Vive tracker.

Because the Avatar VR only returns one quaternion per finger (except for the thumb), I had to think of a way to distribute the orientation along all three phalanges: First, the Euler angles are calculated from the

quaternion[qua]

$$\begin{aligned}\alpha &= \arctan\frac{2(q_0q_1 + q_2q_3)}{1 - 2(q_1^2 + q_2^2)}\\ \beta &= \arcsin(2(q_0q_2 - q_3q_1))\\ \gamma &= \arctan\frac{2(q_0q_3 + q_1q_2)}{1 - 2(q_2^2 + q_3^2)}\end{aligned}$$

where α is the roll angle, β the pitch angle and γ the yaw angle, and the quaternion can be written as (q_0, q_1, q_2, q_3). For implementation, one has to use the `atan2` function, because `arctan` only returns values between $-\frac{\pi}{2}$ and $\frac{\pi}{2}$.

The `NDAPI` quaternions live in a space where the x-axis points to the right, the y-axis points upwards, and the z-axis points into the picture. In terms of geometry, the coordinates are negatively oriented. One might know this as the "left hand rule".

However, `vr_ctrl_panel` is oriented with the negative z-axis pointing out of the picture (positively oriented, "right hand rule"). This results in opposite senses of rotation around the x- and y-axes in the two coordinate systems, so q_1 and q_2 from `NDAPI` need to be negated before use with `cgv`. Then roll corresponds to bending the finger (flexion / extension), pitch to a left-right-motion (abduction / adduction) and yaw to a twisting motion humans can hardly perform with their fingers (pronation / supination).

Since the interphalangeal joints act as revolute joints, only a roll component can be applied to them. As shown in the code below, the roll angle is distributed according to three floats (`rot_split`). After some experimenting, $(.5, .5, .25)$ is an option for these numbers that gives a good approximation of most actual hand poses. It corresponds to phalanx rotation during grabbing. Yaw and pitch are completely executed in the metacarpophalangeal joint.

```
vec3 x(1, 0, 0), y(0, 1, 0), z(0, 0, 1);
recursive_rotations[finger][PROXIMAL] = palm_rotation
        * quat(z, yaw) * quat(y, pitch) * quat(x, rot_split.x() * roll);
recursive_rotations[finger][INTERMED] = quat(x, rot_split.y() * roll);
recursive_rotations[finger][DISTAL] = quat(x, min(1.4f, rot_split.z() * roll));
```

2.3 Project Idea and Structure

To give the VR user interface some context rather than just moving boxes, I decided to design it as a conn panel on the USS Voyager (Star Trek). The term *conn* is short for *control and navigation*, meaning the panel is used to stear the ship. The classes used to implement this and their interaction are shown in figure 2.5.

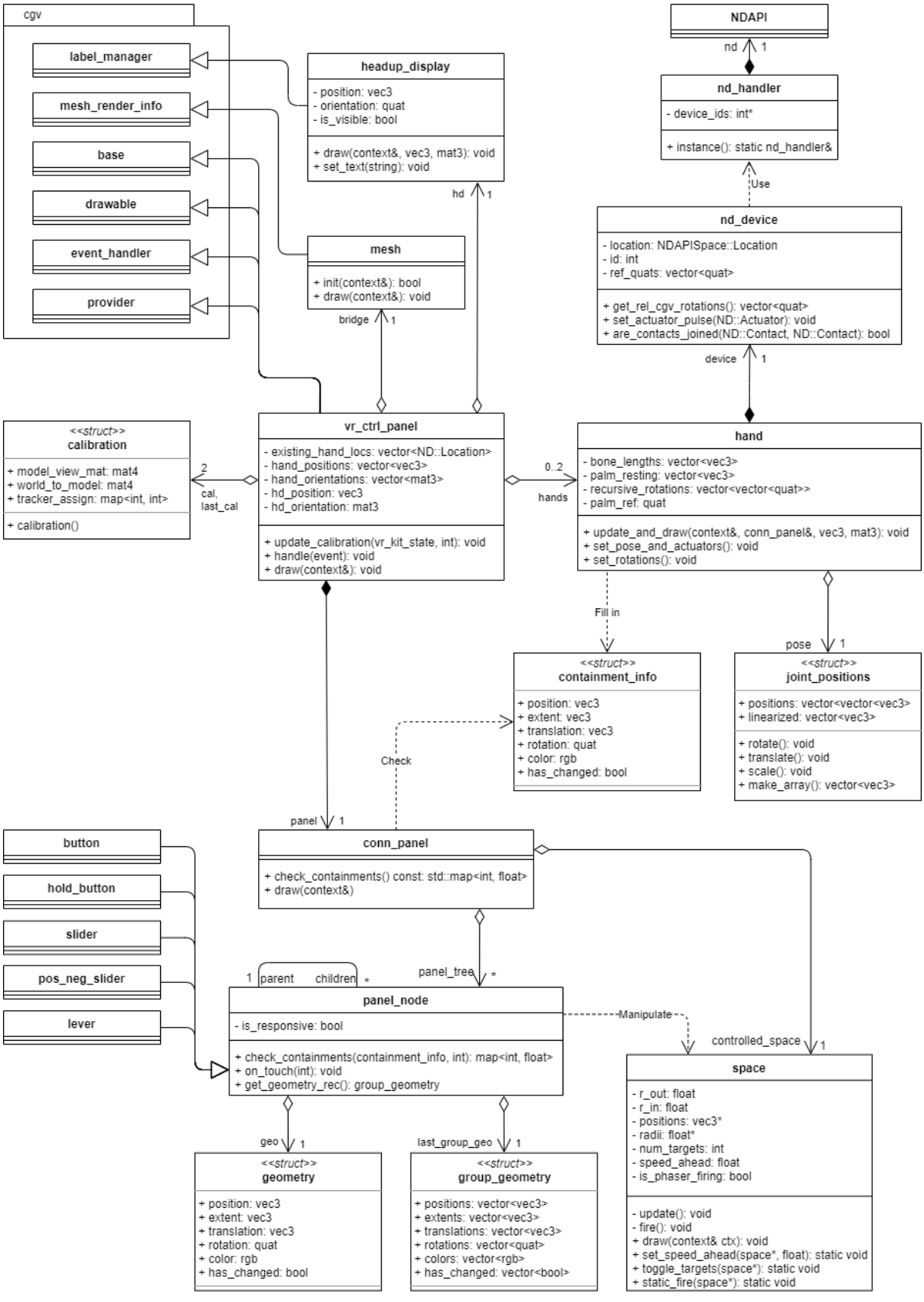

Figure 2.5: Class diagram of `vr_ctrl_panel`, only most relevant elements shown

2.3.1 Main class

The main class and entry point carries the same name as the plugin itself. It is derived from the `cgv` classes `base`, `drawable`, `event_handler` and `provider`, and is used for scene management and interaction with the framework functionalities.

Its capability to handle `vr_pose_events` is used to catch tracker poses and HMD poses (position and orientation) which are forwarded to the `hands` (see section 2.2) and `head_up_display` (see part 2.3.6) respectively during the `draw()` call.

It distributes `draw()` commands among all relevant members (`hand`, `conn_panel`, `mesh`, and `headup_display`). In the process, it passes on the necessary arguments which ensures laziness: recalculations of geometry and containment checks are only done when they are necessary.

This class further manages the calibration routine (see section 2.4). It is the only class registered via object registration.

2.3.2 Bridge

The `mesh` class renders the Voyager bridge. It uses the basic functionality of `mesh_render_info` provided in `cgv` to load and draw. A triangular mesh was provided by Chainsaw_NL and Star trek Meshes (see Copyright). The faces belonging to the viewscreen were deleted to enable a view to the outside.

2.3.3 Space, Targets and Phasers

Around the bridge, space is simulated by a spherical shell filled with stars implemented in `space`. The user never actually changes position in model space. Instead, stars are moved in the opposite direction of the simulated motion. The speed ahead can be set via the following method:

```
static void set_speed_ahead(space* s, float val)
{
        s->speed_ahead = val * s->max_speed_ahead;
}
```

The method needs to be static so it is possible to set it as callback method in objects outside this class. Analogous methods exist for all three rotational speeds. This class also manages targets whose visibility can be toggled with `toggle_targets()` and that can be eliminated with phasers (laser canons) via the `static_fire()` method.

More details and the geometry behind this class are described in section 2.5.

2.3.4 Control Panel

The actual interface is built and drawn by `conn_panel`. This passes the `controlled_space` and a callback function on to each `panel_node` during construction and the `containment_info` coming from a `hand` during `check_containments()`.

In its `draw()` method, `conn_panel` queries the current panel geometry with `panel_tree->get_geometry_rec()` and renders the result with a `box_renderer` provided by `cgv`. The `conn_panel` is positioned right on top of the mesh's conn.

Each `panel_node` is represented as a box or combinations of boxes placed relative to their parent element. During an `on_touch()` call, the non-trivial derived classes (`button`, `hold_button`, `slider`, `pos_neg_slider` and `lever`) use their callback function to manipulate the `controlled_space`.

2.3.5 Hands

Interaction with the Avatar VR is managed by the singleton `nd_handler` which can be used to pass function calls through to an instance of `NDAPI`. This is frequently done in `nd_device`, a class for querying sensor data from the gloves and converting it for better compatibility with `cgv` and `vr_ctrl_panel`, e.g. the sign flip explained at the end of section 2.2.

Finally, the representation of the user's hands is implemented in `hand`. It keeps track of several points and joints the details of which are described in section 2.2. During a `draw()` call, `vr_ctrl_panel` passes a pointer to its `conn_panel` to each `hand` which then passes on information about the current hand geometry wrapped as `containment_info` to the `conn_panel` for containment check. Each `panel_node` containing some hand part can then react with its `on_touch()` method. A `map<int, float>` describing the contained positions and suggested vibration strengths is returned to the hand, enabling it to react as well.

2.3.6 Headup Display

To convey written information to the user, a rectangular white region showing black text can be displayed in front of their eyes. This is implemented in `headup_display` which uses `label_manager` provided by `cgv`. Its visibility can be controlled by setting an empty text (invisible) or a non-empty text (visible).

Whenever the display is invisible, its `draw(context& ctx, vec3 p, mat3 ori)` call simply returns. Otherwise, its position and orientation are updated so it is rendered .6 units in front of and .1 units above the user's eye position:

```
vec3 vs_hmd = ori * vec3(.0f, .1f, -.6f);
```

```
position = pos + vs_hmd;
orientation = ori;
```

2.4 Calibration

To make the use of `vr_ctrl_panel` in different rooms and setups possible, a calibration routine is required. It follows the state diagram shown in figure 2.6. Generally, joined contacts are interpreted in the following way:

- thumb + index: acknowledge
- thumb + middle: decline
- palm + index: choice 1
- palm + index: choice 2

The routine can be activated by joining index and thumb of one hand for three seconds. The hand requesting calibration is saved. The calibration routine does not react to the contacts of the other hand. This is done for reasons of implementation and because users found it natural to control the calibration with a single hand. The current calibration is saved so the user can return to it after aborting.

While in the "requested" stage, the headup display shows a countdown until calibration. After that, none of the objects in the scene are rendered anymore. The user is asked whether the their position should be taken from the HMD or set manually. In case of the latter, one can tap thumb and index above their head to set the position from the current tracker pose.

After that, the hands are rendered again and a countdown of $3s$ is displayed. The user is instructed to hold their hands straight with the fingers pointing forward. During this countdown, the hands and the model view matrix are constantly recalibrated as the following pseudo code shows:

```
vec3 panel_origin = tracker_pos_average;
vec3 new_z = user_pos - panel_origin;
new_z.normalize();
float angle_y = angle between new_z and (0, 0, 1);

// panel_origin becomes coordinate origin
mat4 model_view_mat = translation(panel_origin)
// -new_z becomes view direction
        * rotation((0, 1, 0), angle_y)
// bridge center becomes coordinate origin
        * translation(panel_pos_on_bridge);
mat4 world_to_model = inv(model_view_mat);
```

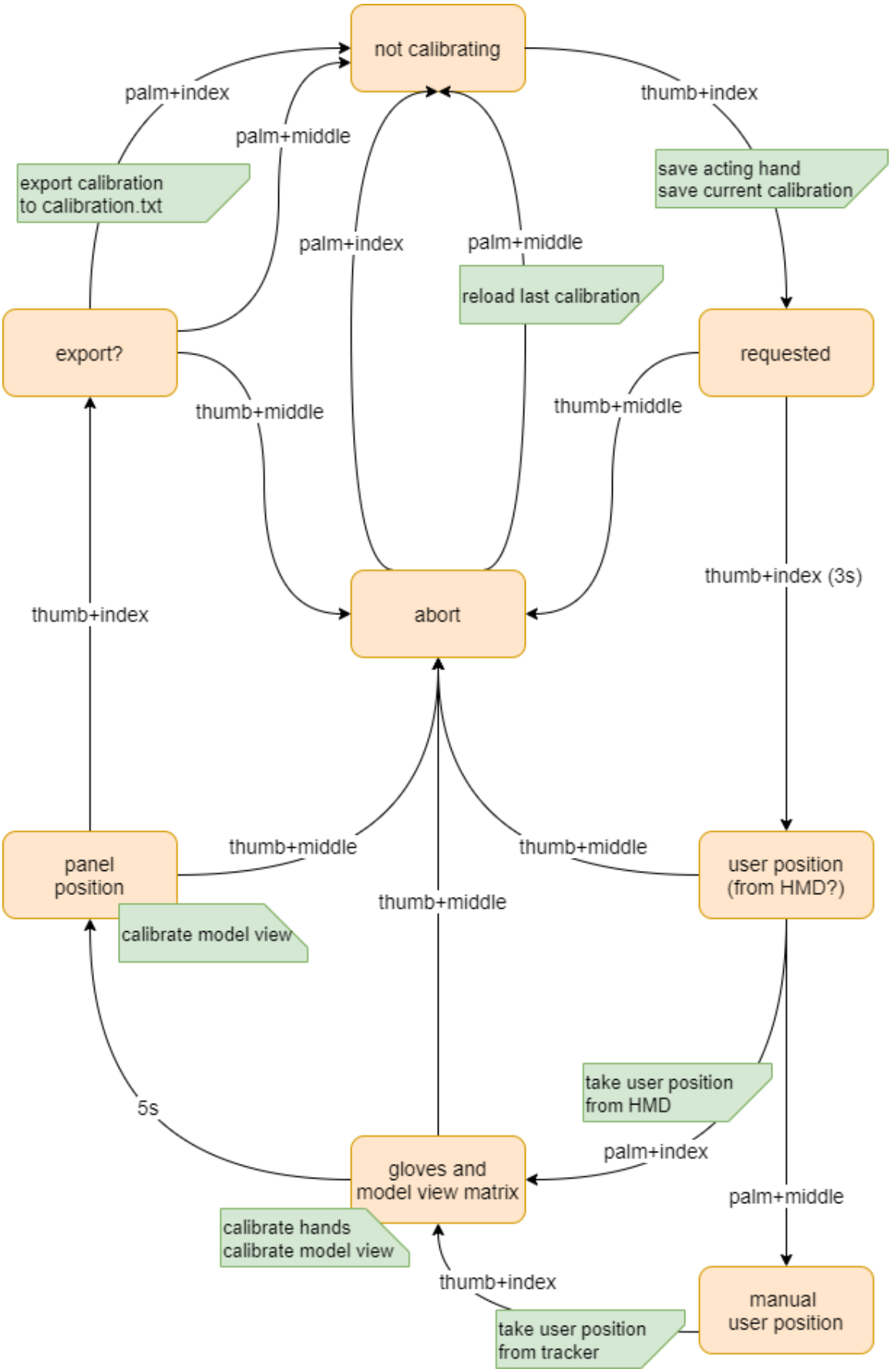

Figure 2.6: State diagram of the calibration routine

```
vector<quat> ref_quats = nd.get_quats_from_sensors();
for (size_t i = 0; i < num_imus; i++)
{
        ref_quats[i] = ref_quats[i].inverse();
}
```

Now, we have the following equalities:

```
new_z == model_view_mat * (0, 0, 1, 1)
(0, 0, 1, 1) == world_to_model * new_z

unit_quat == ref_quats[i] * nd.get_quats_from_sensors()[i]    // for all i
```

The tracker positions are now always transformed to model space by multiplication with `world_to_model` and the quaternions from the sensors are multiplied with the `ref_quats` before use. Therefore, the current calibration pose is assumed as the new "unit", meaning it looks like a trivial pose.

Finally, the conn panel reappears close to the hands. One can continue to adjust the panel position by moving their hands until satisfied. A final acknowledgement by tapping index and thumb ends the calibration. It can then be exported to a file which is automatically loaded at plugin start.

Between two calibration stages, a short feedback pulse is generated by all actuators simultaneously to notify the user of the change. When the calibration is finished, a final pulse runs through the actuators successively.

At any time, the calibration can also be aborted by joining thumb and middle finger which results in three short actuator pulses. One can then choose to return to the previous calibration or keep the partially altered one.

The whole process is communicated to the user on the headup display. It appears with the initial countdown and disappears when returning to the "not calibrating" stage.

2.5 Space, Targets and Phasers

A schematic of the spherical shell used to simulate space is shown in figure 2.7. The outer radius determines the overall size of the sphere. A spherical region around the user that does not contain any stars is defined by the inner radius. This should include the complete bridge mesh to assure stars are only visible to the user on the view screen. Congruent with other parts of the plugin, the flight and view direction points along the negative z-axis.

Stars are rendered as small spheres whose radii follow a normal distribution. The shell is initialized with a constant number of stars with uniformally distributed positions. It saves the forward and angular speeds

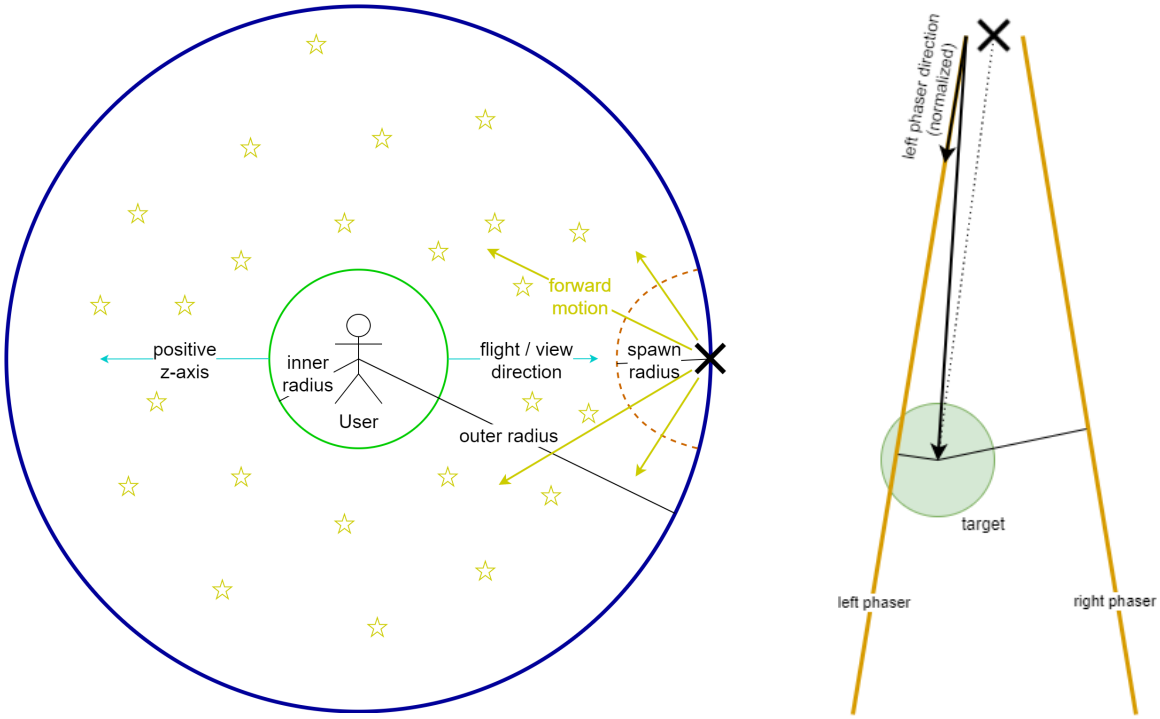

(a) Shell with stars around the user

(b) Target phaser interaction

Figure 2.7: Schematics of the geometry behind the `space` class, see text for explanations

as float values. During a `draw()` call, the method `update()` calculates new positions for all stars. It can be summarized as follows:

for all stars **do**
  Move star away from origin
  if star is outside of shell **then**
    Respawn star
  else
    Rotate star around user
  end if
end for

To somewhat simplify the math behind this calculation, I used the point on the outer hull right in front of the user as origin for the shell space, instead of the center of the shell. The origin is marked with a cross in figure 2.7. A model view matrix then translates the shell to model space.

When moving dead ahead (angular speeds are zero), stars are moved along the yellow "forward motion" arrows in figure 2.7a. The bigger the angle between their position vector and the positive z-axis, the slower they move. More precisely, the length of a star's position vector is increased by the product of the

cosine of the angle between the position vector and the positive z-axis, and the general distance it has covered, calculated from `speed_ahead` and the time since the last update.

If a star moves outside the outer hull of the shell, its position is re-initialized randomly somewhere on a sphere of the spawn radius around the origin. It cannot be simply set to the origin because it needs a direction and the spawn radius should not be too small in order to avoid the impression of stars spawning very densly. Stars moving into the free sphere around the user are mirrored at the user. As this only happens when a forward motion is applied, the star then keeps moving away behind the user.

An additional rotation is realized by simply rotating the stars around the user. After some experimenting, I realized the spawn sphere needs to be rotated inversely around the user as well to achieve a realistic experience and because otherwise, the newly spawned stars converge to a line at slow forward motion and fast rotations.

Because they behave quite similar to the stars, the targets are managed in `space` as well. Their positions are updated as described for the stars. Additionally, their radii are continously adjusted as in the following pseudo code:

```
// value between 0 (at user_pos) and 1 (at outer shell)
float dist_frac = target_pos_rel_to_user.length() / r_out;
// value between 0 (at outer shell) and 1 (at user_pos)
dist_frac = 1 - dist_frac;
// realistic size change
dist_frac = sqrt(dist_frac);
// scale to basic target radius
target_radius_loc = dist_frac * target_radius;
```

This results in a radius of 0 at the outer shell and in a radius of `target_radius` at the user position which is never reached due to mirroring at the inner shell. The targets are not active at plugin start, meaning they are neither updated nor rendered. They can be activated using `toggle_targets()` and deactivated with the same method.

When the `fire()` method is called, phasers are rendered as cones running from the left and right of the view screen to the left and and right of the origin (cross in figure 2.7) where there radius becomes 0. This gives the impression of infinite rays. All targets are checked if they have been hit as shown in the schematic in figure 2.7b (viewed from above) and the following pseudo code:

```
vec3 target_rel_to_left = target_pos - left_phaser_end;
vec3 orth_proj = dot(target_rel_to_left, left_phaser_dir) * left_phaser_dir;
float dist = (target_rel_to_left - orth_proj).length();
bool hit = dist < target_radius_loc;
```

In figure 2.7b, the dotted line corresponds to `target_pos`, the long arrow to `target_rel_to_left` and the

short arrow to the normalized vector `left_phaser_dir`.

If a target has been hit, it is mirrored at the user position removing it from the view screen.

3 Evaluation

3.1 Participating Subjects and Preparation

For the purpose of a user study, I chose two Star Trek Fans (female, 21 and male, 48; called *Trekkies*) and two people not familiar with the franchise (both female, 49 and 11; called *Non-Trekkies*). All of them were instructed how to wear the Avatar VR and the HMD, and had approximately $15min$ to familiarize themselves with the environment, i.e. the conn panel, wearing the HMD, moving through space and eliminating targets.

3.2 Qualitative Evaluations and Suggestions

The subjects were then asked for their opinion and suggestions regarding the design and behavior of the plugin which are summarized below:

- As an essential part of the whole project the haptic feedback strength was adjusted in discussion with the subjects. After that, all subjects regarded the feedback when touching a virtual surface as "strangely realistic" or similar. I then applied different vibration strengths for various panel components which was evaluated as "unrealistic" and "confusing", so I went back to the original approach of a single vibration strength throughout the whole panel. A good value for this strength set as `level` in the `NDAPI` method `set_actuator_pulse()` seems to be .1.

  When asked to reach through the conn panel, they described a sense of intuitive hesitation because their brain had apparently somewhat accepted the physical barrier formed by the virtual panel.

- The target color was changed from red to green increasing the contrast to the orange phasers. The phaser color, position, and direction was adjusted to match the Trekkies impression of a phaser from the movies.

- The "Toggle Targets" button was changed to stay green while the targets are active.

- In the initial implementation, the sliders on the left side of the panel had been designed to react only to touches close to their current setting. This was meant to give the impression of a slider rather

than buttons. However, the participants found it hard to match the current setting which resulted in problems with changing the slider value. This was adjusted so the user can tap anywhere on the slider to immediately change its value. A field was added in the middle of the slider that can be used to set its value exactly to 0.

- Instructions on the headup display during calibration lead to misunderstandings and miscalibrations. They were discussed with the users and adjusted until agreed upon.
- Irritation was expressed when the panel reappeared during calibration because the user's hands ranged into the panel triggering continuous vibration feedback. I added a vector `hand_vs_panel_for_calibration` in the `calibration` struct which moves the panel below the hands during calibration to avoid this.
- The size of the targets represented by `target_radius` above was adjusted until the subjects found it challenging, but possible to eliminate them.

The calibration is necessary because the Avatar VR does not give sufficiently accurate measurements for a period longer than a few minutes. Since the device apparently accumulates quaternions from instantaneous acceleration rates, the resulting rotations tend to diverge quickly from the actual hand pose. This effect is significant if the device was moved even slightly during its intrinsic calibration at startup time and becomes stronger when executing movements with high accelerations, e.g. shaking.

Glossary

framework provided by the chair of computer graphics and visualization at TU Dresden; foundation for the graphics softare developed in this thesis. 2, 7, 8

plugin developed in this thesis. 2, 9, 10, 14, 16

`vr_ctrl_panel`

Avatar VR haptic glove used in this thesis. 2, 6, 10, 17

distal interphalangeal joint joint connecting an intermedial phalanx to a distal phalanx. 2, 10

distal phalanx finger bone farthest from the palm of the human hand, shown in figure 2.2a. 2, 10, 11, 13, 18

head mounted device device worn in front eyes for immersive visualization. 2, 7, 19

intermedial phalanx finger bone of the human hand between proximal phalanx and distal phalanx, shown in figure 2.2a. 2, 10, 11, 18

intertial measurement unit technical device for measuring rotation or acceleration. 2, 3, 11, 19

metacarpal set of bones in the palm of the human hand, shown in figure 2.2a. 2, 10, 11, 18

metacarpophalangeal joint joint connecting a metacarpal to a proximal phalanx. 2, 10, 11, 13, 14

NeuroDigital producer and trademark owner of the Avatar VR. 2, 19

proximal interphalangeal joint joint connecting a proximal phalanx to a intermedial phalanx. 2, 10

proximal phalanx finger bone closest to the palm of the human hand, shown in figure 2.2a. 2, 10, 18

Vive VR system; tracker and headset used in this thesis. 2, 7

Acronyms

HMD head mounted device. 2, 7, 8, 16

IMU intertial measurement unit. 2, 3, 11

ND NeuroDigital. 2, 7, 11, 12

VR Virtual Reality. 2, 3

Bibliography

[KS18] Nayan M. Kakoty and Manalee Dev Sharma. Recognition of sign language alphabets and numbers based on hand kinematics using a data glove. *Procedia Computer Science*, 133:55 – 62, 2018. International Conference on Robotics and Smart Manufacturing (RoSMa2018).

[lea] Introducing the skeletal tracking model. accessed 18 Aug 2020.

[LHT+19] Yang LI, Jin HUANG, Feng TIAN, Hong-An WANG, and Guo-Zhong DAI. Gesture interaction in virtual reality. *Virtual Reality & Intelligent Hardware*, 1(1):84 – 112, 2019.

[MRB+19] Julien Maitre, ClÃ©ment Rendu, KÃ©vin Bouchard, Bruno Bouchard, and SÃ©bastien Gaboury. Basic daily activity recognition with a data glove. *Procedia Computer Science*, 151:108 – 115, 2019. The 10th International Conference on Ambient Systems, Networks and Technologies (ANT 2019) / The 2nd International Conference on Emerging Data and Industry 4.0 (EDI40 2019) / Affiliated Workshops.

[nd] Neurodigital technologies, s. l.

[qua] Conversion between quaternions and euler angles. accessed 19 Aug 2020.

[SEBL06] Fredrik Sebelius, L Eriksson, Christian Balkenius, and T Laurell. Myoelectric control of a computer animated hand: A new concept based on the combined use of a tree-structured artificial neural network and a data glove. *Journal of medical engineering & technology*, 30:2–10, 02 2006.

[SRL05] Fredrik C.P. Sebelius, Birgitta N. Rosén, and Göran N. Lundborg. Refined myoelectric control in below-elbow amputees using artificial neural networks and a data glove. *Journal of Hand Surgery*, 30(4):780–789, Jul 2005.

[Sut65] Ivan E. Sutherland. The ultimate display. In *Proceedings of the IFIP Congress*, pages 506–508, 1965.

[WGL+19] Dangxiao WANG, Yuan GUO, Shiyi LIU, Yuru ZHANG, Weiliang XU, and Jing XIAO. Haptic display for virtual reality: progress and challenges. *Virtual Reality & Intelligent Hardware*, 1(2):136 – 162, 2019.

[ZWW+18] Yukai Zheng, Dangxiao Wang, Ziqi Wang, Yu Zhang, Yuru Zhang, and Weiliang Xu. Design of a lightweight force-feedback glove with a large workspace. *Engineering*, 4(6):869 – 880, 2018.

Acknowledgments

I’d like to thank...

Copyright Information

Voyager Bridge Mesh

Acquired from `https://www.trekmeshes.ch/` on 20 June 2020.

This mesh remains the property of Chainsaw_NL and Star trek Meshes. It however may be used to create images and scenes for non-profit use only.

Any images produced with this mesh do NOT have to be credited to the mesh author. But it would be nice.

Star Trek and Enterprise are copyright Paramount Pictures.